

Efficient, Dynamic Locomotion through Step Placement with Straight Legs and Rolling Contacts

Stefan Fasano¹, James Foster^{1,2}, Sylvain Bertrand¹, Christian DeBuys³, and Robert Griffin^{1,2,3}

Abstract—For humans, fast, efficient walking over flat ground represents the vast majority of locomotion that an individual experiences on a daily basis, and for an effective, real-world humanoid robot the same will likely be the case. In this work, we propose a locomotion controller for efficient walking over near-flat ground using a relatively simple, model-based controller that utilizes a novel combination of several interesting design features including an ALIP-based step adjustment strategy, stance leg length control as an alternative to center of mass height control, and rolling contact for heel-to-toe motion of the stance foot. We then present the results of this controller on our robot Nadia, both in simulation and on hardware. These results include validation of this controller’s ability to perform fast, reliable forward walking at 0.75 m/s along with backwards walking, side-stepping, turning in place, and push recovery. We also present an efficiency comparison between the proposed control strategy and our baseline walking controller over three steady-state walking speeds. Lastly, we demonstrate some of the benefits of utilizing rolling contact in the stance foot, specifically the reduction of necessary positive and negative work throughout the stride.

I. INTRODUCTION

The ability to walk quickly and robustly is a fundamental requirement for legged robots to be useful for real-world tasks. While much of the promise of humanoid robots lies in their potential ability to traverse complex, discontinuous surfaces, they still must be able to quickly and efficiently go from point to point over relatively flat ground. Humans perform both locomotion styles very well, with the ability to pick out and execute specific contact sequences when walking over complex terrain, while equally capable of walking down a hallway or over fields with little thought given to the precise contact location. While much of our previous work has centered around the former, i.e. locomotion over rough terrain using specific contacts in the world [1, 2], in this paper we present a controller designed to quickly, efficiently, and blindly walk over relatively flat ground.

Stable walking is a challenging problem due to the high dimensionality, underlying nonlinearity, limited control authority, and hybrid nature of the locomotion dynamics. The dominant approach has thus been the use of reduced-order and simplified models, most notably with the linear inverted

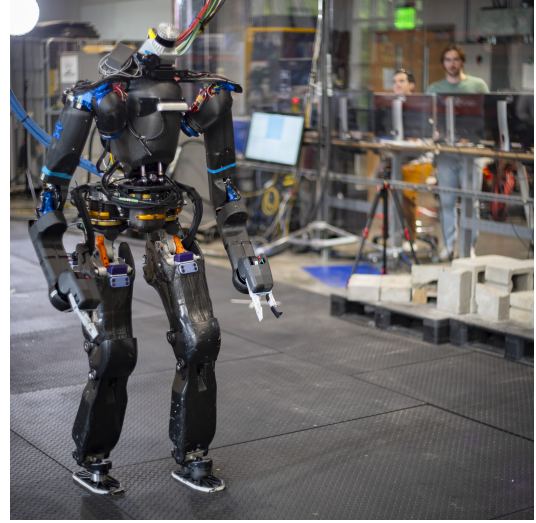


Fig. 1: Our humanoid robot, Nadia, during forward walking hardware tests of the Quickster walking controller.

pendulum (LIP) model [3, 4] and its permutations like zero-moment point [5], capture point [6, 7], and divergent component of motion [8]. More generally, gross robot quantities such as the Center of Mass (CoM) position and velocity [9] or the net angular momentum [10] are controlled with inverse dynamics solvers used to generate joint-level commands from these quantities [1, 11, 12]. A commonly cited issue with these models, though, is that some of the simplifying assumptions tend to reduce the efficiency of the gait, and omit salient features of the dynamics.

To address these limitations, alternatives have been utilized, such as Hybrid Zero Dynamics (HZD) [13, 14], where nonlinear optimization is used to design gaits as periodic orbits in the state space of a hybrid dynamics model. This gait is enforced via feedback linearization [15] or inverse dynamics controllers augmented with control Lyapunov functions [16]. However, in online applications, HZD approaches typically require the introduction of additional control heuristics, and have a limited set of available motions due to the reliance on the offline library of periodic gaits [15]. In a similar vein, trajectory optimization has shown very promising results, especially for long-horizon, complex motion generation [17, 18, 19]. Similar to HZD, though, these motions are typically limited by their reliance on offline computation. The real-time equivalent, whole-body model predictive control (MPC) [20, 21], is emerging as an attractive option for dynamic locomotion, but is often stymied in achieving real-time control rates by the computational complexity of the underlying optimal control problem.

This work was funded through ONR Grant N00014-19-1-2023, NASA Grant 80NSSC20M0197, and DAC Cooperative Agreement W911NF-21-2-0241.

¹Author with the Institute for Human and Machine Cognition

²Author with the University of West Florida

³Author with Boardwalk Robotics, Inc.

Email : {sfasano, jfoster, sbertrand, rgriffin}@ihmc.org, christian.debuys@boardwalkrobotics.com

In this paper, to enable fast, efficient walking, we design the Quickster controller, which focuses on the necessary step placement to achieve a desired CoM velocity while employing additional features for improving efficiency. We utilize the Angular Linear Inverted Pendulum (ALIP) model to determine the necessary step locations to walk at a desired speed [22]. Our 29 degree of freedom humanoid robot, Nadia (see Fig. 1), has considerable distal mass (48% below the pelvis, and 20% below the knees), which generates substantial angular momentum when walking at higher speeds, deviating heavily from the simplified LIP dynamics. However, the ALIP model is shown to incorporate this angular momentum well into its dynamics. To control the height of the robot, we choose to regulate only the stance leg length, rather than the CoM height directly, allowing walking with straighter legs than the classical LIP gaits [23]. To further increase efficiency, we introduce a heel-to-toe rolling contact motion of the Center of Pressure (CoP), which has been observed in biological systems to increase walking efficiency [24]. Additionally, we opt to use only feed-forward CoP control, as opposed to performing any ankle control for balance due to the relatively limited control authority provided by CoP feedback compared to step adjustment when walking at higher speeds. Using this controller, Nadia is able to walk stably at 0.75 m/s and recover from external disturbances.

The main contributions of this paper are:

- Validation of a simple ALIP-based step adjustment controller on a full-size humanoid robot.
- Strategy for directly controlling the stance leg length as opposed to CoM height, and exploration of how this affects the validity of the ALIP-based step adjustment controller.
- Introduction of a novel rolling contact strategy based on biological system observations, and investigation of the efficiency improvements this approach provides.

II. BACKGROUND

The LIP model represents the robot as a point mass that moves at a constant height above the ground, and exerts all its forces through a point foot. This leads to the CoM dynamics:

$$\ddot{\mathbf{x}} = \frac{g}{\Delta z} (\mathbf{x} - \mathbf{r}_{cop}), \quad (1)$$

where \mathbf{x} is the CoM position in x-y, \mathbf{r}_{cop} is the CoP position in x-y, g is gravity, and Δz is the height of the CoM above the ground. This is often written assuming no height acceleration as $\ddot{\mathbf{x}} = \omega^2 (\mathbf{x} - \mathbf{r}_{cop})$, where $\omega = \sqrt{\frac{g}{\Delta z}}$ is the natural frequency of the inverted pendulum. From these dynamics, we can find the solution as

$$\begin{bmatrix} \mathbf{x}(T) \\ \dot{\mathbf{x}}(T) \end{bmatrix} = \begin{bmatrix} c(\omega\Delta T) & \frac{1}{\omega} s(\omega\Delta T) \\ \omega s(\omega\Delta T) & c(\omega\Delta T) \end{bmatrix} \begin{bmatrix} \mathbf{x}(t) \\ \dot{\mathbf{x}}(t) \end{bmatrix}, \quad (2)$$

where $\Delta T = T - t$, c and s are cosh and sinh, respectively, and we assume \mathbf{r}_{cop} is the origin.

The ALIP model proposes an alternative rate state, where the angular momentum about the contact point, L_y for the x

component, is used [22]. This then changes the dynamics to

$$\begin{bmatrix} \dot{x} \\ \dot{L}_y \end{bmatrix} = \begin{bmatrix} 0 & \frac{1}{m\Delta z} \\ mg & 0 \end{bmatrix} \begin{bmatrix} x \\ L_y \end{bmatrix}, \quad (3)$$

which has the solution

$$\begin{bmatrix} x(T) \\ L_y(T) \end{bmatrix} = \begin{bmatrix} c(\omega\Delta T) & \frac{1}{m\Delta z\omega} s(\omega\Delta T) \\ m\Delta z\omega s(\omega\Delta T) & c(\omega\Delta T) \end{bmatrix} \begin{bmatrix} x(t) \\ L_y(t) \end{bmatrix}. \quad (4)$$

This formulation has the distinct advantage of encoding the angular momentum about the CoM into the state estimate, breaking the assumption of a point mass in the LIP model. The generation of angular momentum is required for the robot to swing its leg, but can typically be ignored due to low swing speeds or low leg inertia. For our robot to achieve faster walking speeds, however, this is not the case, so consideration of angular momentum in the robot dynamics is essential. As shown in [22], this ALIP model provides a better estimate of the velocity at the end of the step when angular momentum is generated, which will greatly improve the performance of controllers based on step placement.

III. CONTROLLER DESIGN

The main purpose of the Quickster controller is to regulate the foot placement to achieve stable walking at a desired speed, while also increasing the locomotion efficiency. This can be done by first using step adjustment to achieve stable closed-loop step-to-step dynamics, with efficiency added through a novel method for controlling the robot's height, while also using heel-to-toe motions of the CoP. These feedback and feedforward objectives are then fed into a whole-body inverse dynamics based QP [1].

A. Step Placement Control

While previous works using the ALIP model for step placement have designed a deadbeat controller such that the robot returns to the desired velocity in a single step [22], or use a simple MPC to do so in multiple steps [25], in this work we prefer to specify control gains by shaping the feedback dynamics. We can observe that the robot is able to change the dynamics in Eq. 4 through selection of the step position relative to the CoM. The feedback law in the forward direction can then be defined as

$$x_{k+1} = -\frac{k_p}{m\Delta z} L_y, \quad (5)$$

which makes the closed loop ALIP dynamics

$$\begin{bmatrix} x_{k+1} \\ L_{y,k+1} \end{bmatrix} = \begin{bmatrix} -k_p\omega s(\omega T) & -\frac{k_p}{m\Delta z} c(\omega T) \\ m\Delta z\omega s(\omega T) & c(\omega T) \end{bmatrix} \begin{bmatrix} x_k \\ L_{y,k} \end{bmatrix}. \quad (6)$$

From here, we employ pole placement to select k_p such that the desired closed-loop eigenvalue, λ , is achieved:

$$k_p = \frac{c(\omega T) - \lambda}{m\Delta z\omega s(\omega T)}. \quad (7)$$

Our selection of λ allows us to distribute balance recovery from step to step, achieving the same deadbeat performance as [22] if $\lambda = 0$.

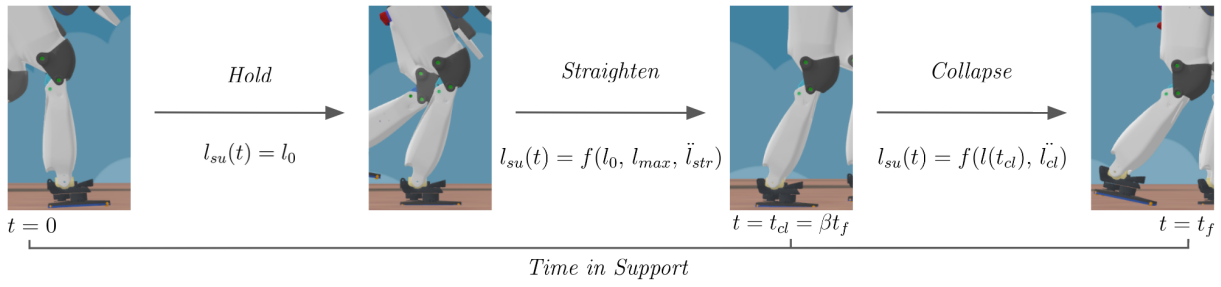


Fig. 2: Stages of stance leg length control. The robot goes first from the *hold* state, where stance leg length is held constant, then into *straighten*, where it is increased at a constant acceleration until a maximum length is achieved, then finally into *collapse*, where the leg length is reduced at a constant acceleration to encourage touchdown.

While the controller in Eq. 7 ensures convergence to a stable zero velocity state at a rate defined by λ , to enable the robot to walk with a given velocity and step width we need to add an offset to our desired footstep. This can be derived from the capture point dynamics [6] as

$$\Delta \xi_{sw} = \frac{\mu}{1 + e^{\omega T}} \quad \text{and} \quad \Delta \xi_{sp}(v_d) = -\frac{v_d T}{e^{\omega T} - 1}, \quad (8)$$

where μ is the desired step width and v_d is the desired speed in x or y . Combining Eqs. 6, 7, and 8, we can derive our step placement control law that will enable the robot to walk with the forward and lateral velocity that we desire:

$$\mathbf{x}_{k+1} = \begin{bmatrix} -k_p \omega x_{ks}(\omega T) - \frac{k_p}{m \Delta z} L_{y,kc}(\omega T) - \Delta \xi_{sp}(\dot{x}_d) \\ -k_p \omega y_{ks}(\omega T) + \frac{k_p}{m \Delta z} L_{x,kc}(\omega T) - \Delta \xi_{sp}(\dot{y}_d) - \Delta \xi_{sw} \end{bmatrix}. \quad (9)$$

B. Height Control through Leg Length

A common technique of many bipedal walking controllers is the direct control of the CoM height dynamics [8, 26]. Often, this is done to satisfy many of the assumptions of the underlying simplified models described in Sec. II. However, kinematic constraints require the variation of height when taking longer steps with straighter legs, both of which are required for more efficient walking [27]. Additionally, by controlling the height rather than the leg length, the controller is susceptible to singularities when the knee is straight. This can be addressed through complex CoM height planning, which often leads to nonlinear formulations [28, 29, 30]. Instead, to simplify the control of height over varied terrain and gain the efficiencies from walking with straighter legs, we propose an alternative paradigm where desired length

changes of the support leg are controlled, rather than the CoM height directly, similar to [23].

Our implementation of indirect walking height modulation through support leg length control can be seen in Fig. 2. On touchdown, the stance leg enters a hold state in which its length remains constant at its initial value l_0 in order to prevent undesirable horizontal CoM deceleration due to premature leg straightening. Once the CoM is within a defined distance of the stance foot, the support leg will begin to straighten to a desired maximum length l_{max} at a constant acceleration \ddot{l}_{str} . The leg will either continue straightening, or remained fully straightened, until a fraction of total stance time β is reached, at which point the leg will collapse at a constant acceleration \ddot{l}_{cl} . The collapse state works concurrently with toe-off at the end of stance such that undesirable CoM height change is avoided. The smooth, periodic CoM height trajectory shown in Fig. 3a highlights this effect. It also serves to encourage touchdown in the event of longer steps, thus preventing the robot from encountering undesirable kinematic and dynamic configurations from late touchdown.

To justify our choice of allowing CoM height fluctuations despite the use of a simplified ALIP model, we analyzed the CoM height and CoM height acceleration of the Quickster controller, and compared them against those of the baseline controller in Fig. 3. The CoM height of both controllers have remarkably similar profiles, shown in Fig. 3a, despite their different approach to height control. This plot also highlights the higher walking height achieved by Quickster's stance leg length control strategy. More important to the assumptions associated with the ALIP model, however, is the CoM height acceleration, shown in Fig. 3b. Both controllers experience similar, sufficiently low height acceleration (less than $0.1g$) during steady-state walking such that the assumption of constant CoM height can still reasonably hold.

C. Definition of Rolling Contact

The introduction of the rolling foot contact, where the CoP goes from the heel to the toe, has been shown to increase the efficiency of the walking gait in biological systems [24]. While the CoP motion in other works has been prescribed by some nominal plan, e.g. [31], biological data suggests that this heel-toe motion is instead a function of CoM position and is invariant to walking speed or time [32], following the motion of a rolling wheel [33] or arced foot [32], as shown

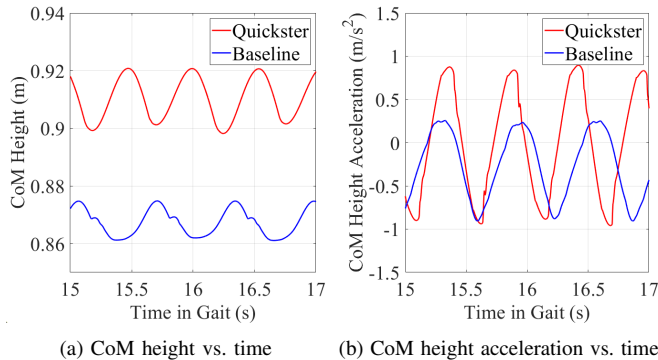


Fig. 3: CoM height and height acceleration comparison between controllers at 0.7 m/s steady-state walking.

on the left in Fig. 4. In this work, we use this more bio-inspired approach, defining the nominal CoP position only as a function of the CoM position, as in the right of Fig. 4.

In the arc-foot rolling contact model, an arc of radius approximately 30% of the leg length (parameterized by α) is added to the foot bottom, which forces the CoP to shift in the direction of the CoM position. When applied to the LIP model, if the CoM is defined relative to the foot, this makes the CoP position relative to the foot

$$\mathbf{r}_{cop} = \alpha \mathbf{x}, \quad (10)$$

leading to the CoP motion shown in Fig. 5, where the CoP goes from the heel to the toe as the CoM moves through the gait. The LIP dynamics from Eq. 1 are then

$$\ddot{\mathbf{x}} = \omega^2 (\mathbf{x} - \alpha \mathbf{x}) \equiv \omega^2 (1 - \alpha) \mathbf{x}. \quad (11)$$

This is equivalent to the system behaving with a time constant of $\omega\sqrt{1-\alpha}$, which, in the context of LIP, means it behaves as a pendulum of height $\frac{\Delta z}{1-\alpha}$. Thus, as this pendulum fraction for rolling contact gets larger (signifying a larger foot), ALIP behaves as a longer pendulum.

In biological data, one of the primary energetic benefits of the arc-foot model comes from reduced losses due to impact at the step-to-step transition [24]. As the LIP and ALIP model of walking prescribes no impact losses, this benefit is lost. However, the use of the rolling contact model applied in Eq. 11 reduces the horizontal ground reaction forces by $(1 - \alpha)$. When the robot is walking forward, it has naturally cyclical forward velocity, where the reaction forces slow and then accelerate the robot from stride to stride. Rolling contact should, theoretically, reduce the “braking” forces applied during each step (reducing negative work), and require decreased “pushing” forces (positive work) to re-accelerate the mass.

The rolling contact CoP position is then used as an objective for the inverse-dynamics based whole-body controller. This, combined with spatial accelerations for the swing foot, the chest orientation, the pelvis orientation, desired knee accelerations from the height control, and desired arm positions, can be used to find desired torques to be executed by the robot’s joints [1].

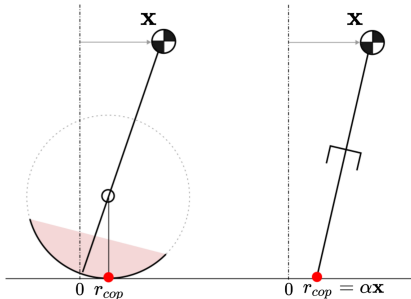


Fig. 4: Left: biological walking can be modeled using arc shaped feet at the base of the inverted pendulum [32]. This reduces the vertical velocity change and corresponding losses due to impact. Right: We also describe rolling contact based on the state, instead using the LIP model, which leads to a modified time constant.

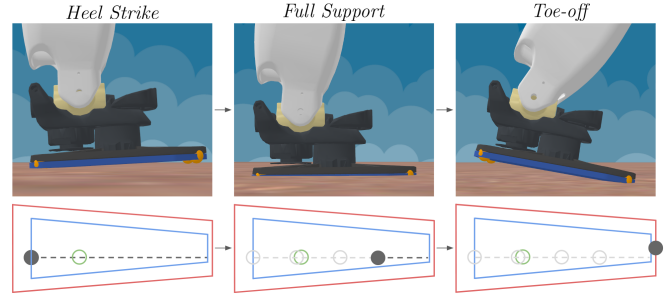


Fig. 5: The full implementation of rolling contact in the Quickster controller including heel strike, full flat-footed support, and toe-off. The non-rolling contact CoP is shown in green. The rolling contact CoP (black) starts at the back of the foot upon heel strike and remains there until toe strike, moves forward in the foot polygon toward the toe in full support, and finally reaches and remains at the front of the foot until toe-off.

IV. RESULTS

To evaluate the efficacy of the Quickster controller in achieving faster, more efficient walking, we conducted several experiments in simulation and on hardware.

A. Satisfaction of Basic Performance Requirements

One of the primary goals of the proposed control strategy is to achieve fast, reliable forward walking that exceeds the speeds capable of our baseline walking controller. Extensive testing and development of this controller resulted in reliable forward walking up to 1.4 m/s in simulation and 0.75 m/s on hardware. While forward walking performance was prioritized during the development of this algorithm, in order to make it as usable as possible, it also must be capable of backwards walking, side-stepping, and turning in place. While no formal speed or efficiency analysis was conducted for these maneuvers, the controller proved capable of performing them reliably throughout numerous tests, both in simulation and on hardware. To test the robustness of Quickster, simulations with blind, unpredictable drops in terrain height steps were conducted at walking speeds of 0.7 m/s, which the controller was capable of traversing. We also conducted disturbance recovery tests on hardware in which the robot was pushed from all directions while walking in place, and while walking forward as shown in Fig. 6. The algorithm proved robust to these perturbations despite its lack of dedicated push recovery functionality, deploying step adjustment to return to a stable limit cycle.

B. Gait Efficiency Comparison Against Baseline

In addition to higher walking speeds, it was our hope that Quickster could also produce an efficient walking gait by considering the angular momentum as part of the step placement dynamics, walking with straighter legs, and utilizing rolling contact in the stance foot. To evaluate this efficiency, we compared the root-mean-squared (RMS) mechanical power of Nadia’s leg pitch joints (hip, knee, and ankle) as well as the sum total RMS mechanical power of all joints during steady-state walking in simulation at three different speeds (0.3 m/s, 0.5 m/s, 0.7 m/s) when using Quickster against those measured when using our baseline controller.

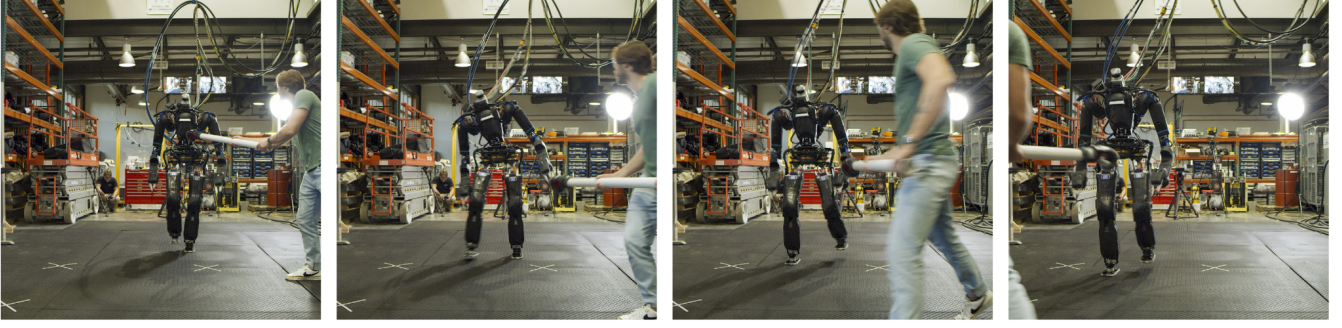


Fig. 6: Push recovery while walking forward. The robot adjusts laterally and backwards, and then continues walking.

These speeds were chosen such that the comparison included the slowest steady-state walking speed nominally used by the baseline controller, as well as the fastest steady-state walking speed that the baseline controller can reliably achieve. The primary comparison was conducted in simulation in order to create the most controlled environment with the least amount of confounding factors or hardware-related constraints such as hardware-specific failures and lack of space for steady-state walking. That said, preliminary hardware experiments were conducted to serve as a reference for the consistency between Quickster's hardware and simulation-based data.

The results of this experiment can be seen in Fig. 7. For nearly all walking speeds and all joints evaluated, the simulation case of the Quickster controller (shown in orange) resulted in less RMS mechanical power expenditure when compared against the simulation case of the baseline controller (shown in blue). These reductions range from 11.6% (ankle joint at 0.5 m/s steady-state), to 46.5% (knee joint at 0.7 m/s steady-state). Moreover, it can be seen

that as walking speed increases, this reduction increases as well. This finding supports our hypothesis that Quickster is not only capable of walking at speeds faster than the baseline, but it also becomes increasingly more efficient in comparison as walking speed increases. There are, however, a few exceptions in which the baseline controller proves more efficient. Firstly, at 0.3 m/s the sum total RMS mechanical power of all joints was slightly higher (2.96%) when using the Quickster compared with that measured when using the baseline. Secondly, Quickster had higher (25.9%) hip power expenditure than the baseline controller, also at a walking speed of 0.3 m/s. It is very likely that the latter finding (higher hip power), is a significant contributor to the former finding (higher total joint power). These increases in RMS mechanical power could be attributed to the speed and quantity of steps required by the Quickster algorithm. While the baseline controller can take fewer and slower steps at slower walking speed thanks to its use of a CoP feedback-based ankle control strategy, Quickster must step with a certain frequency since step placement is the way in which it maintains control authority over the system dynamics. At faster walking speeds, however, both controllers are required to take quicker steps, and Quickster's better inclusion of angular momentum along with its use of straighter legs result in a consistently more efficient gate. This experiment also revealed that Quickster's hardware results (shown in yellow) were relatively consistent with what was measured in simulation, implying that the simulation-based comparison between it and the baseline controller could conceivably be translated to hardware with similar outcomes.

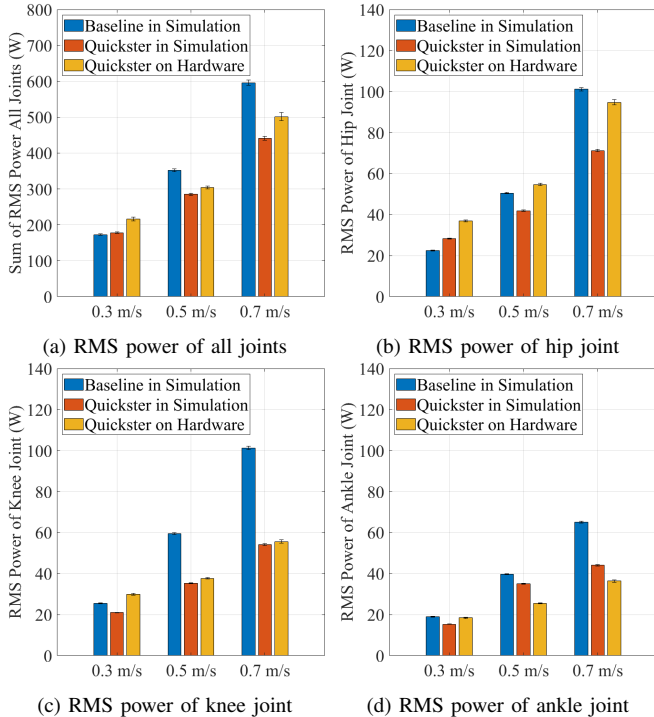


Fig. 7: Comparison of RMS mechanical power expenditure at three steady-state walking speeds.

C. Evaluation of Rolling Contact Benefits

Another potential contribution to the efficiency of Quickster's gait is its use of stance-foot rolling contact. To evaluate the effectiveness of this feature, steady-state walking at 0.7 m/s in simulation was conducted with rolling contact enabled and disabled. A nominal, median steady-state step starting with the touchdown of the current stance foot, and ending with the touchdown of the next stance foot, was chosen to perform this comparison, with results shown in Fig. 8. In the top plots, the CoM forward velocity is plotted as a function of percent of stride. It can be seen that for both cases, there is a deceleration in the beginning of the step corresponding with ground contact of the current stance foot, followed by an acceleration of the CoM as it passes over the foot,

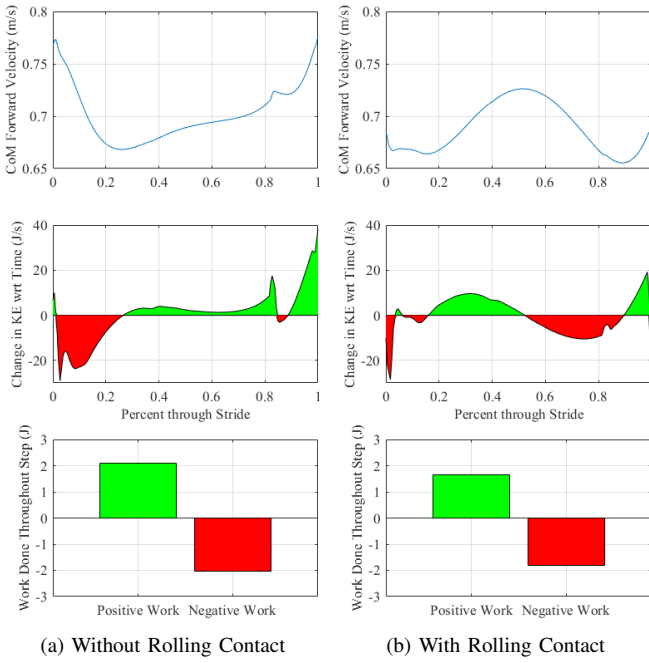


Fig. 8: Comparison of a single, median step during steady-state walking in simulation at 0.7 m/s with rolling contact turned on (right) and with it turned off (left).

followed by an additional sharper acceleration of the CoM around 82% of the way through the stride as a result of toe off. The aforementioned accelerations and decelerations of the CoM can be correlated to positive and negative work done on the robot at different points throughout the stride. This information can be seen in the middle plots which shows the time derivative of the CoM’s kinetic energy as a function of percent of stride. Everything above zero in this plot represents positive work done by the robot (shown in green), and everything below zero represents negative work done by the robot (shown in red). The total amount of positive and negative work done over the course of the stride is shown in the bottom bar graphs of Fig. 8.

This comparison revealed that disabling rolling contact results in a larger CoM deceleration occurring over a longer period of time at the beginning of stride as a result of touchdown. This finding can be attributed to two things. Firstly, in the rolling contact case the location of the CoP at touchdown is closer to the CoM. Secondly, as the CoP rolls forward towards the toe of the stance foot when using rolling contact, the distance between the CoM and CoP decreases in comparison to that same distance when rolling contact is disabled. In both cases, according to LIP dynamics this results in smaller negative and positive CoM accelerations, respectively. However, based on our controller definition, and as can be seen in Fig. 8, the controller does not behave with the force profile of the LIP. In ALIP dynamics, as is used in our controller, this phenomenon results in a smaller moment arm about the contact point for the gravitational force to act upon, causing less change in the angular momentum. The result of these phenomena is less negative work being done on the robot after touchdown, which translates to less positive work required by the controller to maintain steady-

state walking. For this particular median step at this walking speed, using rolling contact provided an 11% reduction in negative work, and a 21% reduction in positive work over the course of the stride. These reductions are not equal because the sampled median step was not perfectly steady-state. For both cases, there was a slight acceleration or deceleration from beginning to end of stance, so net work was not exactly 0 for either one as it would be in ideal steady-state walking.

V. CONCLUSIONS AND FUTURE WORK

For humanoid robots to be effective, they must be able to quickly and efficiently navigate through their environment. In this work, we sought to develop a controller that enables this fast locomotion while increasing the efficiency of the gait. To do so, we designed a walking controller that achieves the desired walking speed using step placement from the ALIP model and pole-placement to control the stability convergence. To improve the efficiency, we introduced a strategy for controlling the leg length directly to walk with straighter legs and implemented a strategy for heel-to-toe motion similar to the one developed in the biomechanics literature based on rolling contacts. We then demonstrate that, using this approach, our humanoid robot Nadia is able to stably walk on hardware at speeds up to 0.75 m/s, as well as stably recover from external disturbances. Additionally, when compared to our baseline walking controller, the proposed approach shows reductions in RMS joint power expenditure that grow as walking speeds increase. Lastly, we show that using rolling contact provides a substantial reduction in the required work for decelerating/accelerating the center of mass for each step.

Several possible extensions exist for future investigation. Firstly, an improved toe-off behavior may improve efficiency by propelling the CoM forward at the end of stance, possibly reducing losses from impact [34], as well as driving the swing foot forward at the transition between support and swing, resulting in a reduction in the amount of work required by the swing leg [35] during the swing phase. This would partly address the high torque and speed demands of the faster swing times required by faster walking speeds. Secondly, we are working on enabling seamless transitions between this controller and our existing walking controller, such that Nadia can traverse its environment in the most appropriate and effective way by switching between the two walking modes. This will then be partnered with environmental models, such as in [36], to enable autonomous mode switching. Lastly, we hope to incorporate emergent arm swing by regulating the whole-body orientation, as proposed in [37], which may further increase walking efficiency [38].

VI. ACKNOWLEDGEMENTS

We would like to thank Nick Kitchel for assistance in experimentation and William Howell for capturing the videos for this work. Also thanks to the mechanical team for keeping the robot in good running condition.

REFERENCES

- [1] T. Koolen, S. Bertrand, G. Thomas, T. de Boer, T. Wu, J. Smith, J. Engelsberger, and J. Pratt, "Design of a momentum-based control framework and application to the humanoid robot Atlas," *International Journal of Humanoid Robotics*, vol. 13, no. 1, 2016.
- [2] R. J. Griffin, G. Wiedebach, S. McCrory, S. Bertrand, I. Lee, and J. Pratt, "Footstep planning for autonomous walking over rough terrain," in *2019 IEEE-RAS 19th International Conference on Humanoid Robots (Humanoids)*. IEEE, 2019, pp. 9–16.
- [3] M. Garcia, A. Chatterjee, A. Ruina, and M. Coleman, "The Simplest Walking Model: Stability, complexity, and scaling," *Journal of Biomechanical Engineering*, vol. 120, no. 2, pp. 281–288, 1998.
- [4] S. Kajita, F. Kanehiro, K. Kaneko, K. Yokoi, and H. Hirukawa, "The 3D linear inverted pendulum mode: A simple modeling for a biped walking pattern generation," in *2001 IEEE/RSJ International Conference on Intelligent Robots and Systems (IROS)*, vol. 1, 2001, pp. 239–246.
- [5] S. Kajita, F. Kanehiro, K. Kaneko, K. Fujiwara, K. Harada, K. Yokoi, and H. Hirukawa, "Biped walking pattern generation by using preview control of zero-moment point," in *2003 IEEE International Conference on Robotics and Automation (ICRA)*, vol. 2. IEEE, 2003, pp. 1620–1626.
- [6] J. Pratt, J. Carff, S. Drakunov, and A. Goswami, "Capture point: A step toward humanoid push recovery," in *2006 6th IEEE-RAS International Conference on Humanoid Robots (Humanoids)*, 2006, pp. 200–207.
- [7] J. Pratt, T. Koolen, T. De Boer, J. Rebula, S. Cotton, J. Carff, M. Johnson, and P. Neuhäus, "Capturability-based analysis and control of legged locomotion, Part 2: Application to M2V2, a lower-body humanoid," *The International Journal of Robotics Research*, vol. 31, no. 10, pp. 1117–1133, 2012.
- [8] J. Engelsberger, C. Ott, and A. Albu-Schäffer, "Three-dimensional bipedal walking control using divergent component of motion," in *2013 IEEE/RSJ International Conference on Intelligent Robots and Systems (IROS)*, 2013, pp. 2600–2607.
- [9] M. G. Boroujeni, E. Daneshman, L. Righetti, and M. Khadiv, "A unified framework for walking and running of bipedal robots," in *2021 20th International Conference on Advanced Robotics (ICAR)*. IEEE, 2021, pp. 396–403.
- [10] A. Herzog, N. Rotella, S. Mason, F. Grimmering, S. Schaal, and L. Righetti, "Momentum control with hierarchical inverse dynamics on a torque-controlled humanoid," *Autonomous Robots*, vol. 40, pp. 473–491, 2016.
- [11] S. Kuindersma, R. Deits, M. Fallon, A. Valenzuela, H. Dai, F. Permenter, T. Koolen, P. Marion, and R. Tedrake, "Optimization-based locomotion planning, estimation, and control design for the Atlas humanoid robot," *Autonomous Robots*, vol. 40, pp. 429–455, 2016.
- [12] S. Feng, X. Xinjiefu, C. G. Atkeson, and J. Kim, "Optimization based controller design and implementation for the Atlas robot in the DARPA Robotics Challenge finals," in *2015 IEEE-RAS 15th International Conference on Humanoid Robots (Humanoids)*. IEEE, 2015, pp. 1028–1035.
- [13] E. R. Westervelt, J. W. Grizzle, and D. E. Koditschek, "Hybrid zero dynamics of planar biped walkers," *IEEE Transactions on Automatic Control*, vol. 48, no. 1, pp. 42–56, 2003.
- [14] J. W. Grizzle, C. Chevallereau, R. W. Sinnet, and A. D. Ames, "Models, feedback control, and open problems of 3D bipedal robotic walking," *Automatica*, vol. 50, no. 8, pp. 1955–1988, 2014.
- [15] J. Reher, E. A. Cousineau, A. Hereid, C. M. Hubicki, and A. D. Ames, "Realizing dynamic and efficient bipedal locomotion on the humanoid robot DURUS," in *2016 IEEE International Conference on Robotics and Automation (ICRA)*, 2016, pp. 1794–1801.
- [16] J. Reher, C. Kann, and A. D. Ames, "An inverse dynamics approach to control Lyapunov functions," in *2020 American Control Conference (ACC)*. IEEE, 2020, pp. 2444–2451.
- [17] C. Mastalli, R. Budhiraja, W. Merkt, G. Saurel, B. Hammoud, M. Naveau, J. Carpentier, L. Righetti, S. Vijayakumar, and N. Mansard, "Crocodyl: An efficient and versatile framework for multi-contact optimal control," in *2020 IEEE International Conference on Robotics and Automation (ICRA)*, 2020, pp. 2536–2542.
- [18] B. Ponton, M. Khadiv, A. Meduri, and L. Righetti, "Efficient multicontact pattern generation with sequential convex approximations of the centroidal dynamics," *IEEE Transactions on Robotics*, vol. 37, no. 5, pp. 1661–1679, 2021.
- [19] M. Posa, C. Cantu, and R. Tedrake, "A direct method for trajectory optimization of rigid bodies through contact," *The International Journal of Robotics Research*, vol. 33, no. 1, pp. 69–81, 2014.
- [20] E. Dantec, M. Naveau, P. Fernbach, N. Villa, G. Saurel, O. Stasse, M. Taix, and N. Mansard, "Whole-body model predictive control for biped locomotion on a torque-controlled humanoid robot," in *2022 IEEE-RAS 21st International Conference on Humanoid Robots (Humanoids)*. IEEE, 2022, pp. 638–644.
- [21] M. Y. Galliker, N. Csomay-Shanklin, R. Grandia, A. J. Taylor, F. Farshidian, M. Hutter, and A. D. Ames, "Planar bipedal locomotion with nonlinear model predictive control: Online gait generation using whole-body dynamics," in *2022 IEEE-RAS 21st International Conference on Humanoid Robots (Humanoids)*. IEEE, 2022, pp. 622–629.
- [22] Y. Gong and J. Grizzle, "One-step ahead prediction of angular momentum about the contact point for control of bipedal locomotion: Validation in a LIP-inspired controller," in *2021 IEEE International Conference on Robotics and Automation (ICRA)*, 2021, pp. 2832–2838.
- [23] R. J. Griffin, G. Wiedebach, S. Bertrand, A. Leonessa, and J. Pratt, "Straight-leg walking through underconstrained whole-body control," in *2018 IEEE International Conference on Robotics and Automation (ICRA)*. IEEE, 2018, pp. 5747–5754.
- [24] P. G. Adamczyk, S. H. Collins, and A. D. Kuo, "The advantages of a rolling foot in human walking," *Journal of Experimental Biology*, vol. 209, no. 20, pp. 3953–3963, 2006.
- [25] G. Gibson, O. Dosunmu-Ogunbi, Y. Gong, and J. Grizzle, "Terrain-adaptive, ALIP-based bipedal locomotion controller via model predictive control and virtual constraints," in *2022 IEEE/RSJ International Conference on Intelligent Robots and Systems (IROS)*. IEEE, 2022, pp. 6724–6731.
- [26] G. Ficht and S. Behnke, "Direct centroidal control for balanced humanoid locomotion," in *Climbing and Walking Robots Conference*. Springer, 2022, pp. 242–255.
- [27] R. J. Griffin, S. Bertrand, G. Wiedebach, A. Leonessa, and J. Pratt, "Capture point trajectories for reduced knee bend using step time optimization," in *2017 IEEE-RAS 17th International Conference on Humanoid Robotics (Humanoids)*. IEEE, 2017, pp. 25–30.
- [28] Z. Huang, Z. Yu, X. Chen, Q. Li, L. Meng, C. Dong, X. Meng, W. Liao, and Q. Huang, "Knee-stretched walking with toe-off and heel-strike for a position-controlled humanoid robot based on model predictive control," *International Journal of Advanced Robotic Systems*, vol. 18, no. 4, 2021.
- [29] B. Park and J. Park, "Heel-strike and toe-off walking of humanoid robot using quadratic programming considering the foot contact states," *Robotics and Autonomous Systems*, vol. 163, 2023.
- [30] S. Dafarra, S. Bertrand, R. J. Griffin, G. Metta, D. Pucci, and J. Pratt, "Non-linear trajectory optimization for large step-ups: Application to the humanoid robot Atlas," in *2020 IEEE/RSJ International Conference on Intelligent Robots and Systems (IROS)*. IEEE, 2020, pp. 3884–3891.
- [31] J. Engelsberger, T. Koolen, S. Bertrand, J. Pratt, C. Ott, and A. Albu-Schäffer, "Trajectory generation for continuous leg forces during double support and heel-to-toe shift based on divergent component of motion," in *2014 IEEE/RSJ International Conference on Intelligent Robots and Systems (IROS)*. IEEE, 2014, pp. 4022–4029.
- [32] A. H. Hansen, D. S. Childress, and E. H. Knox, "Roll-over shapes of human locomotor systems: effects of walking speed," *Clinical Biomechanics*, vol. 19, no. 4, pp. 407–414, 2004.
- [33] T. McGeer, "Passive dynamic walking," *The International Journal of Robotics Research*, vol. 9, no. 2, pp. 62–82, 1990.
- [34] A. D. Kuo, J. M. Donelan, and A. Ruina, "Energetic consequences of walking like an inverted pendulum: step-to-step transitions," *Exercise and Sport Sciences Reviews*, vol. 33, no. 2, pp. 88–97, 2005.
- [35] M. Meinders, A. Gitter, and J. M. Czerniecki, "The role of ankle plantar flexor muscle work during walking," *Scandinavian Journal of Rehabilitation Medicine*, vol. 30, no. 1, pp. 39–46, 1998.
- [36] B. Mishra, D. Calvert, S. Bertrand, S. McCrory, R. Griffin, and H. E. Sevil, "GPU-accelerated rapid planar region extraction for dynamic behaviors on legged robots," in *2021 IEEE/RSJ International Conference on Intelligent Robots and Systems (IROS)*, 2021, pp. 8493–8499.
- [37] Y.-M. Chen, G. Nelson, R. Griffin, M. Posa, and J. Pratt, "Integrable whole-body orientation coordinates for legged robots," *arXiv preprint arXiv:2210.08111*, 2023.
- [38] S. H. Collins, P. G. Adamczyk, and A. D. Kuo, "Dynamic arm swinging in human walking," *Proceedings of the Royal Society B*:

Biological Sciences, vol. 276, no. 1673, pp. 3679–3688, 2009.